Available online at www.sciencedirect.com

ScienceDirect

Proceedings of the Combustion Institute 000 (2018) 1–8

Proceedings of the Combustion Institute

www.elsevier.com/locate/proci

On laminar premixed flame propagating into autoigniting mixtures under engine-relevant conditions

Mahdi Faghih [a], Haiyue Li [a], Xiaolong Gou [b], Zheng Chen [a,*]

[a] *SKLTCS, Department of Mechanics and Engineering Science, College of Engineering, Peking University, Beijing 100871, China*

[b] *School of Power Engineering, Chongqing University, Chongqing 400044, China*

Received 30 November 2017; accepted 9 June 2018
Available online xxx

Abstract

Usually premixed flame propagation and laminar burning velocity are studied for mixtures at normal or elevated temperatures and pressures, under which the ignition delay time of the premixture is much larger than the flame resistance time. However, in spark-ignition engines and spark-assisted compression ignition engines, the end-gas in the front of premixed flame is at the state that autoignition might happen before the mixture is consumed by the premixed flame. In this study, laminar premixed flames propagating into an autoigniting dimethyl ether/air mixture are simulated considering detailed chemistry and transport. The emphasis is on the laminar burning velocity of autoigniting mixtures under engine-relevant conditions. Two types of premixed flames are considered: one is the premixed planar flame propagating into an autoigniting DME/air without confinement; and the other is premixed spherical flame propagating inside a closed chamber, for which four stages are identified. Due to the confinement, the unburned mixture is compressed to high temperature and pressure close to or under engine-relevant conditions. The laminar burning velocity is determined from the constant-volume propagating spherical flame method as well as PREMIX. The laminar burning velocities of autoigniting DME/air mixture at different temperatures, pressures, and autoignition progresses are obtained. It is shown that the first-stage and second-stage autoignition can significantly accelerate the flame propagation and thereby greatly increase the laminar burning velocity. When the first-stage autoignition occurs in the unburned mixture, the isentropic compression assumption does not hold and thereby the traditional method cannot be used to calculate the laminar burning velocity. A modified method without using the isentropic compression assumption is proposed. It is shown to work well for autoigniting mixtures. Besides, a power law correlation is obtained based on all the laminar burning velocity data. It works well for mixtures before autoignition while improvement is still needed for mixtures after autoignition.

Keywords: Premixed flame; Autoignition; Laminar burning velocity; Propagating spherical flame; Engine-relevant condition

* Corresponding author.
E-mail addresses: cz@pku.edu.cn, chenzheng@coe.pku.edu.cn (Z. Chen).

https://doi.org/10.1016/j.proci.2018.06.058
1540-7489

1. Introduction

The laminar burning velocity (LBV), S_u, is defined as the velocity at which an adiabatic, planar, unstretched, premixed flame propagates relative to the unburned gas [1]. It is one of the most important parameters of a combustible mixture. Usually, LBV is measured for mixtures at normal or elevated temperatures and pressures, under which the ignition delay time of the premixture is much larger than the flame resistance time. However, in traditional spark-ignition engines (SIE) and spark-assisted compression ignition (SACI) engines, the end-gas in the front of premixed flame is close to autoignition. Under engine-relevant conditions, the ignition delay time of fuel/air mixture can reach 0.01–1 ms, which is comparable to the flame residence time. Therefore, it is of interests to study premixed flame propagating into autoigniting mixtures under engine-relevant conditions.

In the literature, most of the studies on laminar premixed flames considered non-autoignitive mixtures with ignition delay time much larger than its flame resistance time. Zeldovich [2] was first found that the burning velocity increases as flames propagates into autoigniting mixtures. Later Clarke [3] categorized the planer flame structure based on the Mach number and investigated the importance of thermal and molecular diffusion based on burning velocity. However, only a few studies considered premixed flame propagating into autoigniting mixtures. For examples, Martz et al. [4] found that the reaction front is controlled by chemistry rather than transport when the initial temperature is above 1100 K Therefore it is the propagation spontaneous ignition front rather than flame front. Ju et al. [5] found that low-temperature chemistry and transport play important roles in flame propagating into autoigniting n-heptane/air mixtures. Habisreuther et al. [6] studied the LBV and laminar flame structure of methane/air mixtures for inlet temperatures from 300 to 1450 K. They found that the flame structure changes greatly when the inlet temperature of the mixture is above its autoignition temperature. Sankaran [7] computed the propagation velocity of a one-dimensional stationary flame in a preheated autoignitive lean H_2/air mixture and found that diffusive transport is non-negligible even when the flame is stabilized by autoignition. Yu et al. [8,9] found that end-gas autoignition can induce strong pressure oscillation. Pan et al. [10] found that low-temperature chemistry plays an important role during flame propagation into an autoigniting mixture. They found that similar to ignition delay, the burning velocity shows the non-monotonic NTC (negative temperature coefficient) behavior. Zhang et al. [11] found that the mixture after low-temperature heat release has much larger LBV than the original mixture. More recently, Krisman et al. [12] proposed a method for estimating a reference burning velocity that is valid for laminar flame propagation at autoignitive conditions.

Unlike previous studies mentioned above, this work focuses on the LBV of autoigniting mixtures under engine-relevant conditions and flame propagation in a confined chamber with pressure rise. Except for our work [5,8–10], the above studies only considered unconfined planar flame propagation at nearly constant pressure. In SIE and SACI engines, the premixed flame propagates in a confined space and the end-gas is continuously compressed to higher temperature and pressure. In this study, we also consider premixed spherical flame propagation into an autoigniting mixture inside a closed vessel. In fact, the constant-volume propagating spherical flame method (CVM) [13] has the advantage in measuring the LBV under engine-relevant conditions [14]. Therefore, it is used here to determine the LBV for autoigniting mixtures.

The objectives of this study are to investigate the transient evolution of premixed flame propagating into an autoigniting mixture and to determine the LBV of autoigniting mixtures under engine-relevant conditions. Stoichiometric dimethyl ether (DME)/air mixture is considered here. Two types of premixed flames are considered in the present simulation. One is the premixed planar flame propagating into autoigniting DME/air without confinement. Therefore the unburned mixture is not compressed to higher temperature and pressure during the flame propagation. The other is premixed spherical flame propagating into autoigniting DME/air inside a closed chamber. Due to the confinement, the unburned mixture is compressed to higher temperature and pressure during the spherical flame propagation. As such, very high initial temperature and pressure close to or under engine-relevant conditions can be reached in the unburned gas.

2. Numerical methods

Both steady and propagating premixed flames are considered in this work. For 1D steady planar flames, they are simulated by CHEMIKIN-PREMIX [15], from which the LBVs are obtained. The gradient and curvature parameters are adjusted so that above 800 grid points are contained in the converged solutions. This ensures the grid independency of LBV. For 1D propagating planar and spherical flames, they are simulated by the in-house code A-SURF [16–18]. A-SURF solves the conservation equations for 1D compressible reactive flow using the finite volume method. The thermal and transport properties and reaction rates are determined by CHEMKIN package incorporated into A-SURF. The detailed description of governing equations and numerical method of A-SURF are presented in [16–18] and thus are not repeated here.

Please cite this article as: M. Faghih et al., On laminar premixed flame propagating into autoigniting mixtures under engine-relevant conditions, Proceedings of the Combustion Institute (2018), https://doi.org/10.1016/j.proci.2018.06.058

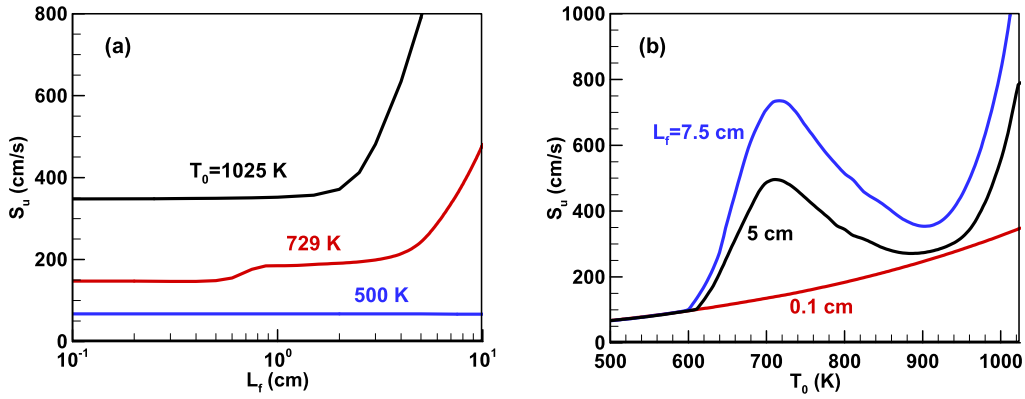

Fig. 1. Change of the LBV with (a) induction length and (b) initial temperature for stoichiometric DME/air at $P_0 = 5$ atm. The results are calculated from PREMIX [15].

Dynamic adaptive mesh [22] is used to efficiently resolve the propagating flame front, which is always covered by finest meshes with the size of 8 μm. Numerical convergence has been checked and ensured by further decreasing the time step and mesh size in simulation and is shown in the Supplementary Document. For the transient planar flame, it propagates in an open space with the computational domain length of 150 cm. For the transient spherical flame, it propagates inside a spherical chamber with the radius of $R_W = 10$ cm unless otherwise specified.

The fuel considered here is DME since it has a well-developed compact chemistry, which can be handled in transient simulation. It also has low-temperature chemistry and NTC behavior. Only stoichiometric DME/air mixture is considered. The detailed chemistry developed by Zhao et al. [19] is used in PREMIX and A-SURF. The performance of this mechanism is compared with the more recent mechanism developed by Wang et al. [20] in the Supplementary Document and nearly the same results are obtained from these two mechanisms. The mixture-averaged model is used to evaluate the mass diffusivities for different species; and a correction term for diffusion velocity is included to ensure compatibility of species and mass conservation equations. It is noted that at certain temperatures and pressures the simulation may not be able to return the burning velocity due to extreme autoignition conditions. Although we cannot determine the bound of these initial conditions, such conditions are avoided in this work.

3. Results and discussion

3.1. Freely propagating planar flame in autoigniting mixture without confinement

First, we consider freely propagating planar flame into an autoigniting mixture without confinement. It is well known that for non-autoignitive mixture, the LBV is an eigenvalue solution and it does not depend on induction length (defined as the distance between the inlet of fresh mixture and the position of steady flame front). However, in autoigniting mixtures, chemical reactions occur during the mixture approaching to the flame front, and the calculated LBV depends on the induction length [2,3,7,12] (note that LBV is still used here though it is not an eigenvalue for autoigniting mixture). This is demonstrated by the results in Fig. 1(a). For $T_0 = 500$ K, the LBV is shown to be independent of the induction length L_f. This is because the ignition delay time at $T_0 = 500$ K is a few order larger than the flame resistance time, and the mixture can be considered as non-autoignitive. For $T_0 = 729$ K, the LBV is shown to increase with L_f, and the curve in Fig. 1(a) is similar to the temperature history for two-stage homogenous ignition process. For $L_f < 0.5$ cm, the first-stage autoignition does not happen and thereby the LBV remains nearly constant, $S_u = 147$ cm/s. Around $L_f = 0.8$ cm, the first-stage autoignition happens before the mixture enters into the flame front and thereby the LBV increases to around 185 cm/s. Around $L_f = 5$ cm, the second-stage heat release starts before the mixture reaches the flame front and the LBV abruptly increases. At large L_f (>10 cm), the flame is stabilized by autoignition, for which dS_L/dL_f is equal to the inverse of the ignition delay time [7,12]. For $T_0 = 1025$ K, the mixture has single-stage autoignition and thereby the LBV is shown to increases abruptly with L_f only around $L_f = 3$ cm.

Figure 1(b) further shows that the LBV depends on the induction length for $T_0 > 600$ K. For $L_f = 5$ and 7.5 cm, the LBV is shown to first increase, then decrease, and finally increase with T_0. This is due to the NTC autoignition behavior caused by low-temperature chemistry. Similar results were also obtained for n-heptane by Pan et al. [10]. However, for a small value of induction length, $L_f = 0.1$ cm, the

Please cite this article as: M. Faghih et al., On laminar premixed flame propagating into autoigniting mixtures under engine-relevant conditions, Proceedings of the Combustion Institute (2018), https://doi.org/10.1016/j.proci.2018.06.058

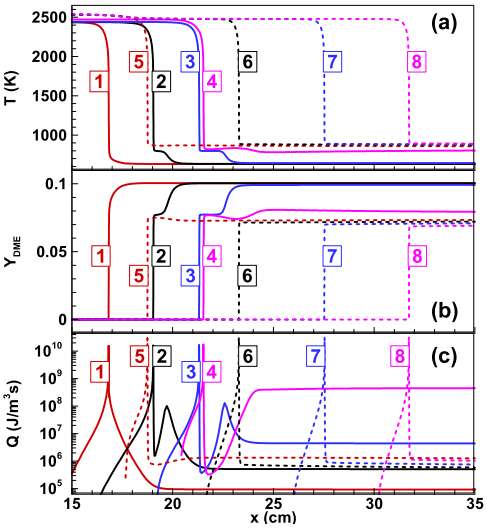

Fig. 2. Temporal evolution of (a) temperature, (b) fuel mass fraction, and (c) heat release rate distributions during premixed planar flame propagating in DME/air with $\phi = 1$, $T_0 = 630$ K and $P_0 = 1$ atm. The time sequence for lines #1∼8 is 25.2, 28, 31.1, 33.1, 34, 40, 45 and 50 ms.

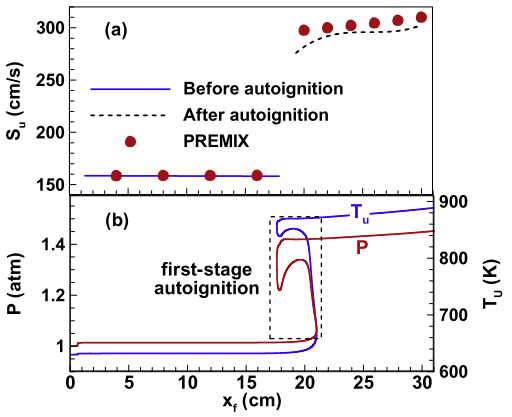

Fig. 3. (a) Laminar burning velocity and (b) pressure and temperature of unburned gas as a function of flame location for DME/air flame with $\phi = 1$, $T_0 = 630$ K and $P_0 = 1$ atm.

LBV is shown to increase monotonically with T_0. Therefore, for autoigniting mixture the LBV should be calculated with small induction length such that the influence of autoignition can be diminished. It is noted that the value of $L = 0.1$ cm is chosen for $P = 5$ atm. At higher pressures, the ignition delay becomes shorter and thereby a value lower than $L = 0.1$ cm needs to be used. Similar conclusion was drawn by Krisman et al. [12].

We then study transient premixed flame propagation in autoigniting DME/air mixture with $T_0 = 630$ K and $P_0 = 1$ atm. This condition is chosen such that two-stage autoignition can be observed. For the planar flame the left boundary is reflective, the right boundary is transmissive and the computational domain length of 150 cm is used. Figure 2 shows the temporal evolution of the temperature, fuel mass fraction and heat release rate distributions. A normal premixed flame is observed at $t = 25.2$ ms (line #1). At $t = 28$ and 31.1 ms (lines #2 and #3), the first-stage autoignition starts to occur in front of the flame and fuel is partially consumed. At $t = 33.1$ ms (line #4), first-stage autoignition occurs in all the unburned mixture, whose temperature is then increased to above 800 K while the fuel mass fraction is reduced to around 7.5%. Due to the pressure rise caused by first-stage heat release in the unburned gas, the flame front propagation is halted and pushed backward (from line #3 to #4 and to #5). Then the premixed flame propagates into autoigniting mixture after first-stage autoignition (from line #5 to #8).

In propagating planar flames, the LBV is equal to the difference between flame propagation speed (dx_f/dt) and the unburned gas flow speed (U_u), i.e., $S_u = dx_f/dt - U_u$. The LBV obtained from the above transient simulation of premixed flame propagation is shown in Fig. 3(a). The LBV calculated by PREMIX is plotted together for comparison. Good agreement is achieved, indicating that the LBV can be calculated accurately in the transient simulation of premixed planar flame propagation in autoigniting mixture. The temperature and pressure of unburned gas are shown in Fig. 3(b). It is noted that the open domain is used in the planar flame simulation and the pressure increases due to autoignition rather than the confinement effect. Before the first-stage autoignition in the unburned gas, the LBV remains constant, $S_u = 158$ cm/s. After the first-stage autoignition in the unburned gas, both the temperature and pressure of unburned gas increase. Consequently the LBV is increased to the range of 275∼295 cm/s. The burning velocity increases here since the autoignition increases the temperature and pressure of unburned mixture which itself enhances the burning velocity. It is noted that this mechanism is different from the "double flame" observed in [11] and it was attributed to flame front propagation into the low-temperature chemistry radical pool.

3.2. Spherical flame propagation in autoigniting mixture with confinement

Then we consider premixed spherical flame propagation in autoigniting DME/air mixture inside a closed chamber.

Figure 4 shows the results for premixed spherical flame propagating in DME/air ($\phi = 1$, $T_0 = 591$ K and $P_0 = 2$ atm) inside a spherical chamber with the radius of $R_W = 10$ cm. At

Please cite this article as: M. Faghih et al., On laminar premixed flame propagating into autoigniting mixtures under engine-relevant conditions, Proceedings of the Combustion Institute (2018), https://doi.org/10.1016/j.proci.2018.06.058

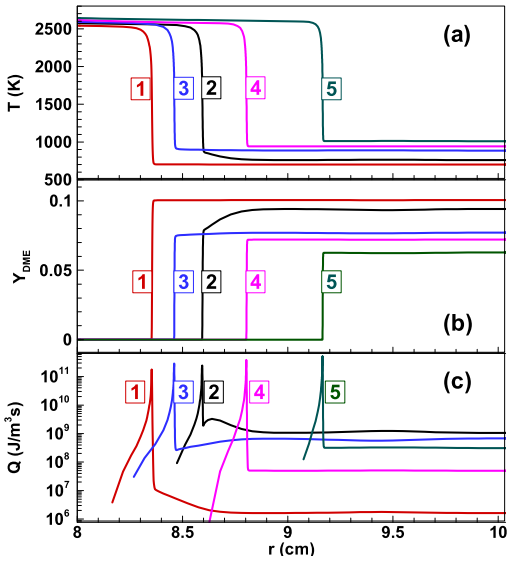

Fig. 4. Temporal evolution of (a) temperature, (b) fuel mass fraction, and (c) heat release rate distributions during premixed spherical flame propagating in DME/air with $\phi = 1$, $T_0 = 591$ K and $P_0 = 2$ atm. The time sequence for lines #1∼5 is 18.1, 19.1, 19.3, 20.1, and 21.1 ms.

$t = 18.1$ ms (line #1), the normal flame propagates and there is no autoignition in the unburned gas. The unburned gas temperature is 701 K due to adiabatic compression by the expanding flame. At $t = 19.1$ ms (line#2), the first-stage autoignition occurs in the unburned gas. The flame front is pushed back by the pressure rise due to the first-stage heat release (from line #2 to line #3), which is similar to that for propagating planar flame (see Fig. 2). Then the spherical flame propagates into the mixture after first-stage heat release (lines #3-#5) and eventually the second-stage autoignition happens in the unburned gas. Figure 4(c) shows that the heat release rate in unburned gas changes non-monotonically with the time. This is due to the occurrence of two-stage autoignition in the unburned gas at $T_0 = 591$ K which is clearly demonstrated in Fig. 5. For $T_0 = 900$ K, only single-stage autoignition happens to the unburned gas. Therefore the normalized heat release rate is shown to monotonically increase with time for $T_0 = 900$ K. For $T_0 = 400$ K, the unburned gas is not autoignitive and thereby the heat release rate is shown to abruptly increase when the flame reaches the wall at $t = t_C$.

Figure 6(a) shows the pressure history during spherical flame propagation in autoigniting DME/air mixture ($\phi = 1$, $T_0 = 591$ K and $P_0 = 2$ atm). As indicated in Fig. 6(a), there are four stages according to pressure evolution. Stage I corresponds to normal flame propagation and the autoignition in unburned gas is nearly negligible since

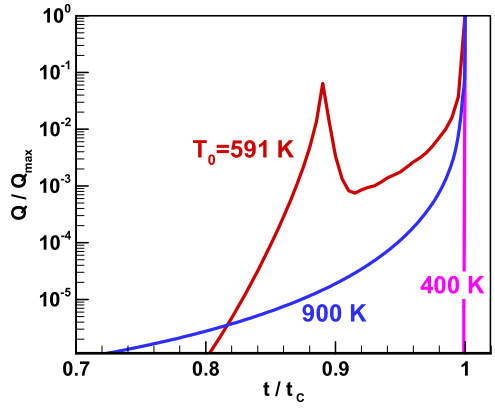

Fig. 5. The evolution of heat release rate in unburned gas near the wall ($R_W = 10$ cm) for DME/air at $\phi = 1$, $P_0 = 2$ atm and different initial temperatures. The heat release rate and time are normalized respectively by the maximum heat release rate and combustion time for each initial temperature.

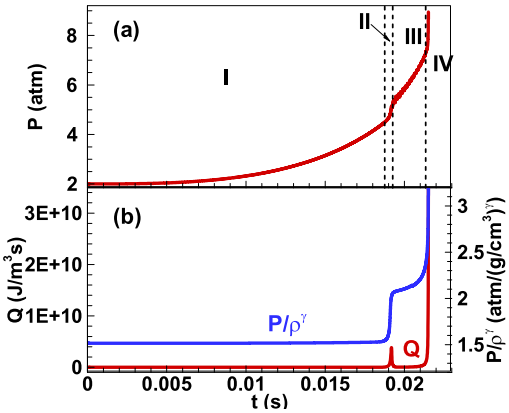

Fig. 6. (a) Pressure history and (b) heat release rate and P/ρ^{γ} in unburned gas near the wall ($R_W = 10$ cm) during premixed spherical flame propagating in DME/air with $\phi = 1$, $T_0 = 591$ K and $P_0 = 2$ atm.

its heat release rate is close to zero as shown in Fig. 6(b). Besides, the unburned gas is compressed isentropically. This is demonstrated by Fig. 6(b) which shows that P/ρ^{γ} remains constant during stage I. In stage II, the first-stage autoignition occurs in the unburned gas and thereby there is obvious pressure rise due to both first-stage autoignition and compression. In stage III, the pressure continuously rises due to compression. Meanwhile, the second-stage autoignition happens, especially at the end of stage III. It is observed in Fig. 6(b) that P/ρ^{γ} continuously increases during stage III and thereby isentropic compression cannot be assumed. Finally, in stage IV global autoignition occurs in the whole

Please cite this article as: M. Faghih et al., On laminar premixed flame propagating into autoigniting mixtures under engine-relevant conditions, Proceedings of the Combustion Institute (2018), https://doi.org/10.1016/j.proci.2018.06.058

unburned mixture and the pressure increases significantly in a very short time.

The constant-volume spherical flame method can be used to obtain the LBV at elevated temperatures and pressures [14]. Under the assumption of isentropic compression of unburned gas, the LBV can be calculated from pressure history according the following correlation [13]:

$$S_u = \frac{R_W}{3}\left(1-(1-x)\left(\frac{P_0}{P}\right)^{1/\gamma_u}\right)^{-2/3}\left(\frac{P_0}{P}\right)^{1/\gamma_u}\frac{dx}{dt} \quad (1)$$

where R_W is the radius of the spherical vessel, P_0 the initial pressure, and γ_u the heat capacity ratio of unburned gas. The burned mass fraction, x, is determined from pressure history through two-zone or multi-zone models in experiments (see [13] and references therein) and it can be calculated directly in simulation. Since isentropic compression of unburned gas was assumed [13] to derive Eq. (1), this correlation is not valid when the unburned mixture doesn't compress isentropically. As shown in Fig. 6(b), isentropic compression is not valid for stages II–IV and thereby Eq. (1) cannot be used to obtain LBV. As shown in the Supplementary Document, the following expression for LBV can be derived without using the assumption of isentropic compression in unburned gas:

$$S_u = \frac{R_W}{3}\left(1-(1-x)\left(\frac{\rho_0}{\rho}\right)\right)^{-2/3}\left(\frac{\rho_0}{\rho}\right)\frac{dx}{dt} \quad (2)$$

in which ρ is the density of unburned gas. For autoigniting mixtures, both the pressure and the unburned gas temperature should be measured. The unburned gas density in Eq. (2) is then obtained from pressure and temperature through the equation of state.

Figure 7 compares the LBV determined by Eqs. (1) and (2). The results from PREMIX are plotted together for comparison. To avoid the domain size dependency in PREMIX calculation, a small induction length is used. In stage I, the isentropic compression of unburned gas holds and thereby the LBV from Eq. (1) is the same as that from Eq. (2), both agreeing well with the PREMIX results. In stages II–IV, the unburned gas is not compressed isentropically since autoignition happens. Therefore, the LBV predicted by Eq. (1) is shown to be different from that predicted by Eq. (2). It is observed that the LBV from Eq. (2) agrees well with that calculated from PREMIX. Therefore, Eq. (2) can be used to obtain LBV for autoigniting mixtures. It is noted that we only consider stoichiometric DME/air here. In the Supplementary Document we also consider lean DME/air mixture with $\phi=0.7$, $T_0=591$ K and $P_0=2$ atm. Similar results and conclusions are obtained.

Whether and when end-gas autoignition occurs is determined by the difference between flame propagation time and ignition delay time. Therefore, the chamber size plays an important role in end-gas autoignition [9]. We conduct simulations of spherical flame propagation in different chamber sizes. Figure 8(a) compares the LBV determined by Eq. (2) with different spherical chamber sizes of $R_W=2.5$, 5, 7.5 and 10 cm. With the increase of chamber size, autoignition happens at relatively low pressure rise [9]. Therefore, the LBV obtained from $R_W=10$ cm is shown to be higher than that from $R_W=7.5$ cm. Besides, for $R_W=2.5$ and 5 cm, only the first-stage occurs in the unburned gas and thereby there is no stage IV. Figure 8(b) depicts the

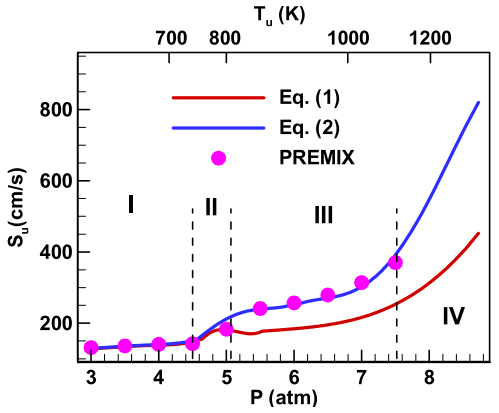

Fig. 7. Evolution of LBV as a function of the increasing unburned mixture pressure, determined by Eq. (1) and Eq. (2) for DME/air mixture with $\phi=1$, $T_0=591$ K and $P_0=2$ atm. The results from PREMIX are plotted together for comparison.

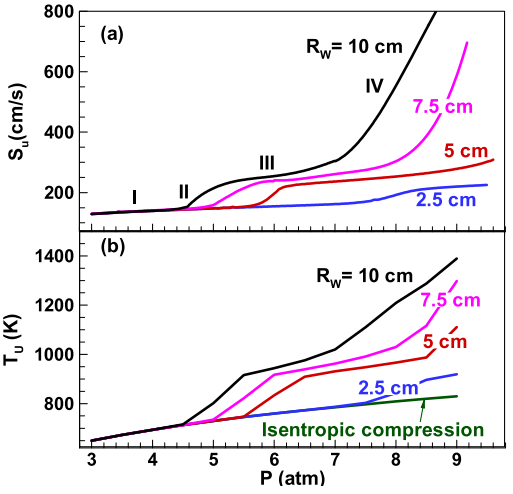

Fig. 8. Change of (a) laminar burning velocity and (b) unburned gas temperature with pressure for DME/air with $\phi=1$, $T_0=591$ K, $P_0=2$ atm. Eq. (2) is used to determine the laminar burning velocity.

Please cite this article as: M. Faghih et al., On laminar premixed flame propagating into autoigniting mixtures under engine-relevant conditions, Proceedings of the Combustion Institute (2018), https://doi.org/10.1016/j.proci.2018.06.058

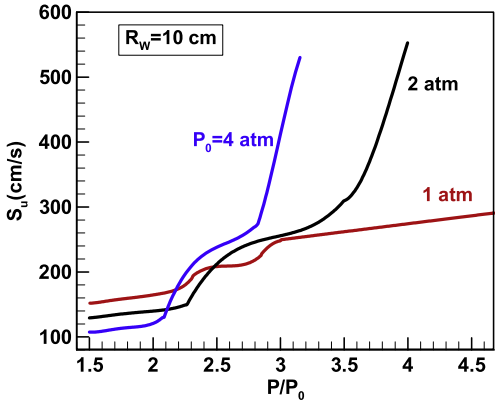

Fig. 9. Laminar burning velocity for spherical DME/air flame with $\phi = 1$, $T_0 = 591$ K and different initial pressures. Eq. (2) is used to determine the laminar burning velocity.

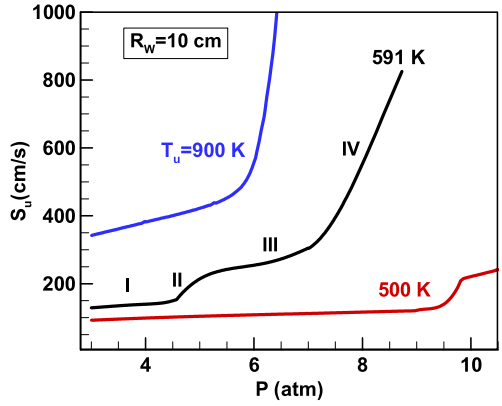

Fig. 10. Laminar burning velocity for spherical DME/air flame with $\phi = 1$, $P_0 = 2$ atm and different initial temperatures. Eq. (2) is used to determine the laminar burning velocity.

corresponding unburned gas temperature for different chamber sizes. It is observed that unburned gas temperature does not follow the isentropic compression once autoignition occurs in the unburned gas. With the increasing trend of autoignition by using larger chamber size, the unburned gas temperature becomes higher and so does the LBV. Therefore, we can get LBV at different intensities of autoignition by using different chamber sizes.

Figure 9 compares the LBV obtained for different initial pressures of $P_0 = 1$, 2 and 4 atm. Since the ignition delay time and flame propagation speed both decrease with the increase of initial pressure, autoignition occurs earlier at higher initial pressure. Before the first-stage autoignition in the unburned gas (i.e., during stage I), the LBV is smaller at higher initial pressure. However, after the first-stage autoignition, the LBV is larger at higher initial pressure. This is due to stronger first-stage heat release at higher initial pressure. It is observed that for $P_0 = 1$ atm, the second-stage autoignition does not happen and thereby there is no sharp increase in LBV for $P_0 = 1$ atm in Fig. 9.

Figure 10 compares the LBV determined for different initial temperatures of $T_0 = 500$, 591 and 900 K. At high initial temperature of $T_0 = 900$ K which is outside the NTC regime, the unburned gas does not have two-stage autoignition. Therefore for $T_0 = 900$ K, there is an abrupt increase of LBV around $P = 6$ atm, which is due to the single-stage autoignition of unburned gas. Though the initial temperatures of $T_0 = 500$ and 591 K are both outside the NTC regime, the temperature of unburned gas increases due to compression and then it can enter the NTC regime. Therefore, for both $T_0 = 500$ and 591 K, the first-stage autoignition happens to the unburned mixture and a step-increase in LBV is observed (i.e., stage II). For $T_0 = 500$ K, the second-stage autoignition does not happen and thereby

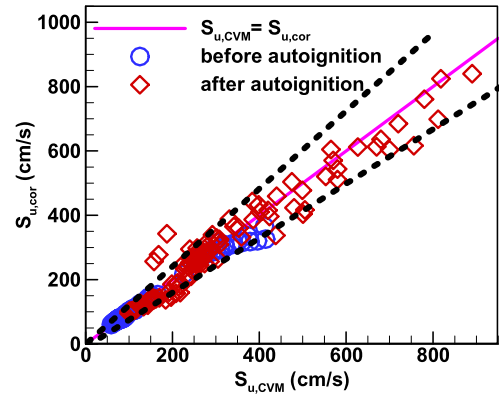

Fig. 11. Comparison of the LBVs predicted by Eq. (3) with those obtained from the constant-volume spherical flame method (CVM). The dashed lines denote the border of 20% deviation of Eq. (3) from CVM.

there is no sharp increase in LBV (i.e., stage IV does not exist).

The above results indicate that the LBV of autoigniting DME/air mixture under engine-relevant temperature and pressure can be obtained from the constant-volume spherical flame method (CVM). All the LBV data can be correlated through the following power law [21]:

$$S_u = S_{u,0}(T_u/T_{u,0})^{\alpha}(P/P_0)^{\beta} \quad (3)$$

where $S_{u,0}$ is the LBV at the reference temperature, $T_{u,0}$ and pressure, P_0. The coefficients α and β are obtained through least-square fitting all LBV data by the power law. They are $\alpha = 3.34$ and $\beta = -0.568$ for the stoichiometric DME/air mixture considered in the present study. Figure 11 compares the LBVs predicted by Eq. (3), $S_{u,\mathrm{cor}}$, and those obtained from transient simulation of spherical flame

Please cite this article as: M. Faghih et al., On laminar premixed flame propagating into autoigniting mixtures under engine-relevant conditions, Proceedings of the Combustion Institute (2018), https://doi.org/10.1016/j.proci.2018.06.058

propagation and Eq. (2), $S_{u,CVM}$. Good agreement is observed, especially for mixtures before autoignition. When autoignition occurs in the unburned mixture, the LBV depends on not only the corresponding temperature and pressure, but also the progress of autoignition, which is demonstrated by results in Fig. 8. Before autoignition the mean deviation of $S_{u,\mathrm{cor}}$ from $S_{u,CVM}$ is 4.1%; while it reaches 10.2% after autoignition. Therefore, the power law in Eq. (3) does not work well for mixture after autoignition. Another parameter characterizing the autoignition progress should be introduced, which deserves further study.

4. Conclusions

Numerical simulations are conducted for premixed planar and spherical flames propagating in autoigniting DME/air mixture. Detailed chemistry and transport are considered. The emphasis is on the laminar burning velocity (LBV) of autoigniting mixtures under engine-relevant conditions. The main conclusions are:

(1) For autoigniting DME/air mixture, the LBV depends on the induction length. The LBV has the behavior similar to the ignition delay time (i.e., non-monotonic change with temperature) when the induction length is 5 or 7.5 cm (see Fig. 1b). To diminish the influence of autoignition on LBV, a small induction length, e.g., 0.1 cm, should be used to calculate LBV.
(2) For spherical flame propagating into autoigniting mixture inside a spherical chamber, the unburned gas is isentropically compressed before the first-stage autoignition happens. Therefore, the traditional method, Eq. (1), can be used to calculate LBV. However, once the first-stage autoignition occurs in the unburned mixture, the isentropic compression assumption does not hold. Consequently, Eq. (2) without isentropic compression assumption should be used to calculate LBV.
(3) The LBVs of autoigniting DME/air mixture at different temperatures, pressures, and autoignition progresses are calculated. It is shown that the first-stage and second-stage autoignition can significantly accelerate the flame propagation and thereby greatly increase the LBV. All the LBV data are fitted by the power law in Eq. (3), which works well for mixtures before autoignition. However, it does not work very well for mixtures after autoignition. Further study is needed and another parameter characterizing the autoignition progress should be introduced.

Acknowledgments

This work is supported by National Natural Science Foundation of China (Nos. 91541204 and 91741126). We thank helpful discussion with Prof. Yiguang Ju at Princeton University.

Supplementary materials

Supplementary material associated with this article can be found, in the online version, at doi:10.1016/j.proci.2018.06.058.

References

[1] G.E. Andrews, D. Bradley, *Combust. Flame* 18 (1972) 133–153.
[2] Y.B. Zeldovich, *Combust. Flame* 39 (1980) 211–214.
[3] J.F. Clarke, *Combust. Flame* 50 (1983) 125–138.
[4] J. Martz, H. Kwak, H. Im, G. Lavoie, D. Assanis, *Proc. Combust. Inst.* 33 (2011) 3001–3006.
[5] Y. Ju, W. Sun, M.P. Burke, X. Gou, Z. Chen, *Proc. Combust. Inst.* 33 (2011) 1245–1251.
[6] P. Habisreuther, F.C.C. Galeazzo, C. Prathap, N. Zarzalis, *Combust. Flame* 160 (2013) 2770–2782.
[7] R. Sankaran, in: 9th U.S. National Combustion Meeting, 2015.
[8] H. Yu, Z. Chen, *Combust. Flame* 162 (2015) 4102–4111.
[9] H. Yu, C. Qi, Z. Chen, *Proc. Combust. Inst.* 36 (2017) 3533–3541.
[10] J. Pan, H. Wei, G. Shu, Z. Chen, P. Zhao, *Combust. Flame* 174 (2016) 179–193.
[11] W. Zhang, M. Faghih, X. Gou, Z. Chen, *Combust. Flame* 187 (2018) 129–136.
[12] A. Krisman, E.R. Hawkes, J.H. Chen, *Combust. Flame* 188 (2018) 399–411.
[13] M. Faghih, Z. Chen, *Sci. Bull.* 61 (2016) 1296–1310.
[14] C. Xiouris, T. Ye, J. Jayachandran, F.N. Egolfopoulos, *Combust. Flame* 163 (2016) 270–283.
[15] R.J. Kee, J. Grcar, M. Smooke, J. Miller, PREMIX: a FORTRAN program for modeling steady laminar one-dimensional premixed flames, Sandia Report. SAND85-8240 (1985).
[16] Z. Chen, M.P. Burke, Y.G. Ju, *Proc. Combust. Inst.* 32 (2009) 1253–1260.
[17] Z. Chen, *Combust. Flame* 157 (2010) 2267–2276.
[18] P. Dai, Z. Chen, *Combust. Flame* 162 (2015) 4183–4193.
[19] Z. Zhao, M. Chaos, A. Kazakov, F.L. Dryer, *Int. J. Chem. Kinet.* 40 (2008) 1–18.
[20] Z. Wang, X. Zhang, L. Xing, L. Zhang, F. Herrmann, K. Moshammer, F. Qi, K. Kohse-Höinghaus, *Combust. Flame* 162 (2015) 1113–1125.
[21] H. Metghalchi, J.C. Keck, *Combust. Flame* 38 (1980) 143–154.
[22] S.Z. Chen, K. Xu, C.B. Lee, Q.D. Cai, *J. Comput. Phys.* 231 (2012) 6643–6664.

Please cite this article as: M. Faghih et al., On laminar premixed flame propagating into autoigniting mixtures under engine-relevant conditions, Proceedings of the Combustion Institute (2018), https://doi.org/10.1016/j.proci.2018.06.058